

Strictly one-dimensional electron system in Au chains on Ge(001) revealed by photoelectron k -space mapping

S. Meyer,¹ J. Schäfer,¹ C. Blumenstein,¹ P. Höpfner,¹ A. Bostwick,² J. L. McChesney,² E. Rotenberg,² and R. Claessen¹

¹Physikalisches Institut, Universität Würzburg, D-97074 Würzburg, Germany

²Advanced Light Source, Lawrence Berkeley National Laboratory, Berkeley, California 94720, USA

(Received 7 February 2011; published 28 March 2011)

Atomic nanowires formed by Au on Ge(001) are scrutinized for the band topology of the conduction electron system by k -resolved photoemission. Two metallic electron pockets are observed. Their Fermi surface sheets form straight lines without undulations perpendicular to the chains within experimental uncertainty. The electrons hence emerge as strictly confined to one dimension. Moreover, the system is stable against a Peierls distortion down to 10 K, lending itself for studies of the spectral function.

DOI: [10.1103/PhysRevB.83.121411](https://doi.org/10.1103/PhysRevB.83.121411)

PACS number(s): 73.20.At, 71.10.Pm, 73.20.Mf, 79.60.-i

Self-organized atomic chains on semiconductors offer a variety of architectures and provide model systems to study exotic physics in a nearly one-dimensional (1D) situation. Representatives include In chains on Si(111),¹ Au on Si(557) and (553),^{2,3} and the recent addition of Au chains on Ge(001).⁴ Such chains with tunable properties are in focus as critical tests of predictions from solid state theory. This pertains, e.g., to the Peierls instability, where a charge density wave (CDW) leads to a metal-insulator transition.⁵ Alternatively, for strictly 1D systems, a correlated electron state known as the Luttinger liquid is proposed,⁶ not found in surface systems thus far.

The key technique to address these issues is angle-resolved photoemission (ARPES). As paramount criterion for a CDW, a nesting condition must exist in a Fermi surface of quasi-1D character, accompanied by energy gaps. CDW formation was reported, e.g., for In/Si(111) at moderate cooling to ~ 200 K.^{1,7} Since fluctuations hinder an ideal 1D system from ordering,⁵ significant interchain coupling is required to stabilize the Peierls phase. In ARPES, a half-filled band with quasi-1D character is identified.¹ The higher-dimensional coupling is enhanced by two additional metallic bands with noticeable lateral dispersion, which are also affected by the gap opening.⁸ Hence, a realistic situation with multiple bands drastically modifies a naive Peierls picture, while inhibiting formation of an exotic 1D electron liquid.

A claim of non-Fermi-liquid physics was made for Au/Si(557) nanowires,² based on an alleged spin-charge separation, yet subsequent ARPES work excluded this by revealing two conventional electron bands.⁹ Moreover, small energy gaps are observed,¹⁰ pointing at a Peierls-type instability. Thus, the search for atomic chains with a highly 1D confined electron system devoid of CDW instabilities is still ongoing. In this respect, noble metal chains on Ge(001) have attracted attention.^{4,11,12} The recently discovered Au chains⁴ have a uniquely elevated architecture and a pronounced spatial separation, suggestive of low interchain coupling. This spurs heightened interest in the resulting degree of electronic 1D character. Scanning tunneling microscopy (STM) investigations can provide at best a qualitative indication.¹³ Yet, except for ambiguous low-statistics data,¹⁴ high-resolution ARPES Fermi surface mapping to address the dimensionality, manifold bands, nesting conditions, and potential energy gaps versus unusual line shapes is missing to date.

In this Rapid Communication, we present ARPES k -space mapping of these chains at 15 K, which reveals an unusual band topology that significantly differs from all previous nanowire systems to our knowledge. It represents a *single-band* system, with two electron pockets on either side of the Brillouin zone. The Fermi surface consists of *parallel lines*, with possible variations from 1D behavior below the detection limit. The incommensurate band filling does not support a simple Peierls scenario, and a CDW is absent in electron diffraction down to 10 K.

Experimentally, Au was deposited onto n -doped Ge(001) at a substrate temperature of $\sim 500^\circ\text{C}$, which induces self-organized nanowire growth.⁴ ARPES at 15 K was performed at the Advanced Light Source at beamline 7.0.1. The total energy resolution with a Scienta R4000 analyzer was set to ~ 30 meV at a photon energy of $h\nu = 100$ eV.

A salient feature of the nanowires, seen in STM [Fig. 1(a)] is that they are raised above the substrate.¹⁵ The lateral spacing amounts to 1.6 nm. Two orientation domains (rotated by 90°) result from terrace steps of the substrate. The Au/Ge(001) chains lend themselves to ARPES studies because they exhibit excellent long-range order, reflected in their $c(8 \times 2)$ low-energy electron diffraction (LEED) pattern.⁴

An overview of the Fermi surface is presented in Fig. 1(b). Note that the square structure solely results from the dual domains; nonetheless the respective sheets are well separated from their rotated counterparts. The $c(8 \times 2)$ surface Brillouin zone (SBZ) in Fig. 1(b) is a stretched hexagon of $\pm 0.42 \text{ \AA}^{-1}$ extending on the 1D axis to the zone boundary (ZB). Photoemission intensities are remarkably suppressed in higher SBZs, which we ascribe to optical transition matrix element effects which can cause significant modulations.¹⁶ Already in this coarse-grid overview one observes a strikingly linear shape of the Fermi surface sheets, to be studied in detail below. This clearly disproves an earlier interpretation as a two-dimensional metallic state.¹⁴

The central cut through $\bar{\Gamma}$ in Fig. 2(a) shows the band situation along the chains. By variation of photon energy the surface character of the bands is identified, and at $h\nu = 100$ eV the Ge bulk bands are tuned away. Two shallow electron pockets are located on either side of $\bar{\Gamma}$. Faint intensity is observed below them at higher binding energies, relating to deeper-lying bands. The band situation near the Fermi surface

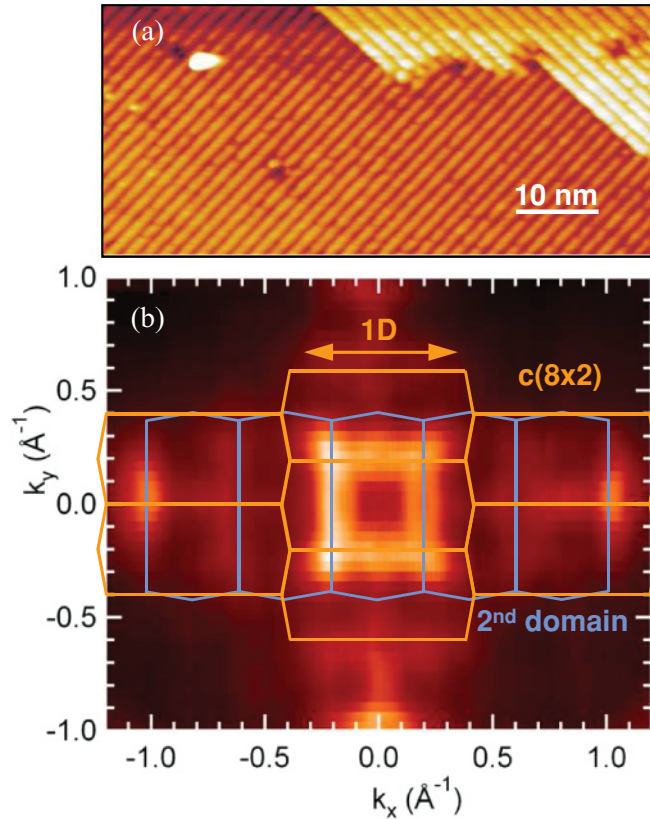


FIG. 1. (Color online) (a) STM image of the Au-induced nanowires (empty states, bias +1.0 V, 1.0 nA), showing two domains from terrace stacking. (b) ARPES Fermi surface overview at $h\nu = 100$ eV, $T = 15$ K from dual-domain sample. The two sheets within the SBZ are rather straight, perpendicular to the corresponding 1D direction. Higher SBZs appear suppressed, which is ascribed to matrix element effects.

of a single nanowire domain, consisting of two troughs formed by the electron pockets, is sketched in Fig. 2(b).

These bands are of roughly symmetric shape with a band minimum at $\sim 0.20 \text{ \AA}^{-1}$, located approximately at half the distance to the ZB. No such surface states are known from bare Ge(001),¹⁷ so they must originate from the chain reconstruction. The Fermi level crossings on either side of $\bar{\Gamma}$ are spaced by $\sim 0.12 \text{ \AA}^{-1}$. The occupied bandwidth is ~ 100 meV, which is small compared to the ~ 500 meV range for In/Si(111),⁸ and the eV range for Au on stepped silicon.¹⁸

In passing on the 1D axis into the second SBZ, the ARPES scan coincides with the SBZ boundary line through \bar{M} , as illustrated in Fig. 2(c). The ARPES data in Fig. 2(d) reveal a parabolic hole band at \bar{M} with weak intensity. A two-dimensional (2D) character is determined from a constant-energy surface, Fig. 2(e); hence it must obey conventional Fermi liquid statistics. This 2D band forms a small hole pocket and exhibits a metallic Fermi edge [see spectra in Fig. 4(d) below]. This *intrinsic* reference is used to precisely determine the *chemical potential* μ (usually termed the Fermi level E_F). This is superior to a metal foil reference due to a possible surface photovoltage of the sample.

It is important to note that the 2D hole band is *not* located directly at the surface. This follows from the tunneling spectroscopy data in Ref. 4, where a 2D density of states (DOS) (which is constant with energy) would lead to a step in the spectrum just above the Fermi level, which is not observed. Thus, the band must be localized in subsurface layers. Such substrate-derived states with hole-like dispersion are well known to occur as interface states in metal-adsorbed Ge (in addition to the adatom surface states), and are located within ~ 10 – 20 layers below the topmost layer.^{19,20}

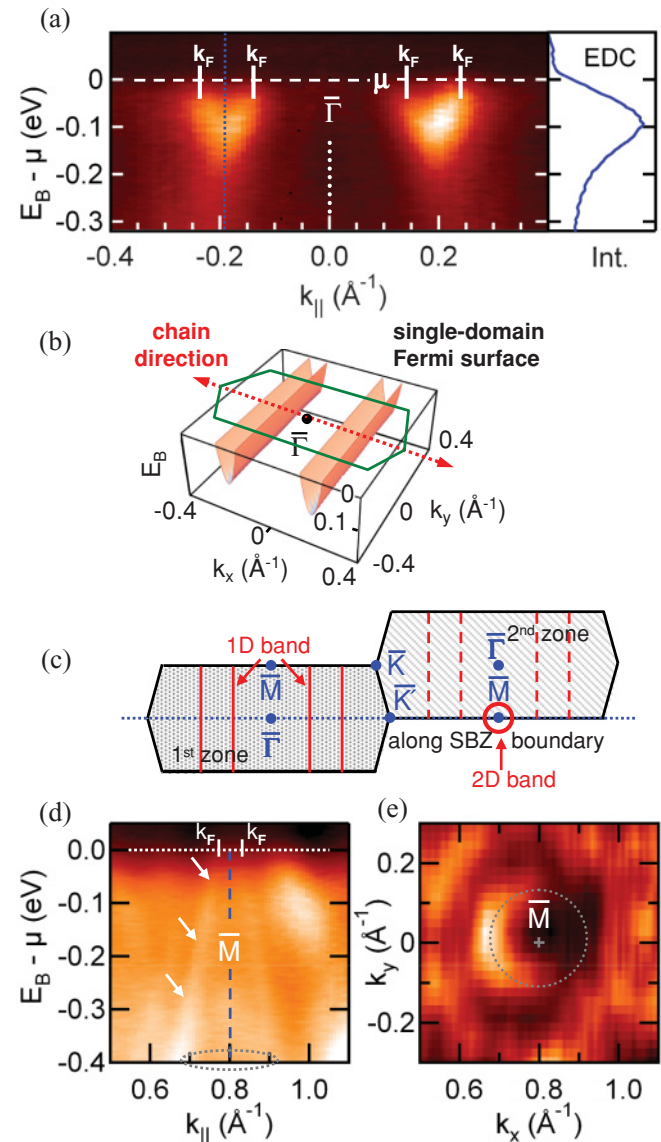


FIG. 2. (Color online) (a) ARPES band map at 100 eV and $T = 15$ K along chain direction through $\bar{\Gamma}$. Two shallow electron pockets are seen [EDC taken at blue (dark gray) dotted line]. (b) Schematic of band situation for single-domain Au chains on Ge(001), consisting of two troughs. (c) Schematic of SBZ alignment. (d) Band map along $\bar{K}' - \bar{M}$ of second SBZ, showing a metallic hole band at \bar{M} used as intrinsic reference for μ . (e) Constant-energy surface at 0.4 eV binding energy, revealing the 2D character of the band at \bar{M} .

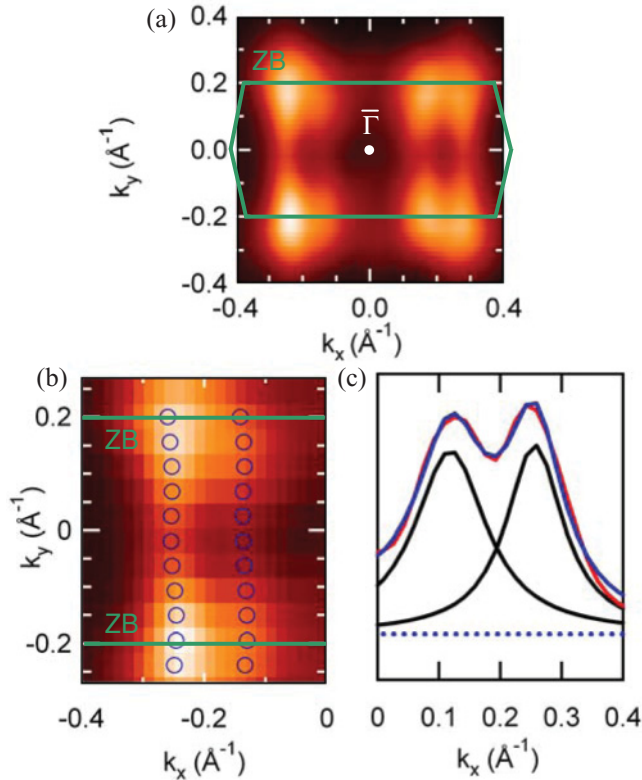


FIG. 3. (Color online) (a) Fermi surface (energy window μ to 30 meV below μ , to compensate for low spectral weight at μ) of sample with domain imbalance. (b) Closeup of Fermi surface data (window μ to 30 meV below μ) with k_F positions from MDC fits [blue (dark) circles]. Variations in the perpendicular k_F lines are absent except for statistical uncertainty. (c) MDC fit for line through $\bar{\Gamma}$, showing two clearly separated k_F 's.

Precise evaluation of the dimensionality is based on k -space mapping of the constant-energy contours near μ , which host the 1D electron liquid. High-statistics Fermi surface data for samples with a domain imbalance (relating to a small incidental crystal miscut), as in Fig. 3(a), can be used to trace the dispersion. On either side of $\bar{\Gamma}$ two ridges corresponding to the Fermi vectors of the electron pocket are identified. The resulting Fermi surface lines appear very straight throughout, notably extending up to the zone boundary. The band filling f is obtained from its relation to the SBZ area as the fraction of occupied k_x range, $f \sim 0.12 \text{ \AA}^{-1}/0.80 \text{ \AA}^{-1} \sim 0.15$ for each pocket, yielding a total band filling of ~ 0.30 .

Quantitative dispersion evaluation must rely on the momentum distribution curves (MDCs). The MDC peaks in the closeup of the Fermi surface, Fig. 3(b), are fitted with Lorentzians to determine the k_F 's. The MDC maxima are well separated, as in the example in Fig. 3(c). This analysis of the dispersion perpendicular to the chains confirms that it is virtually perfectly straight. The remaining small scatter in the k_F positions reflects the statistical uncertainty of the MDC analysis of the two closely adjacent peaks. For each k_F contour line the accuracy of the analysis amounts to $\delta k = 0.004 \text{ \AA}^{-1}$, determined as the standard deviation of 110 independent MDC fits of several data sets. This value provides a tight upper boundary for possible undulations within the Fermi surface.

In contrast, significantly larger Fermi surface curvatures are reported for, e.g., Au on Si(553) (undulation $\delta k \sim 0.03 \text{ \AA}^{-1}$) which indicates a substantial coupling between neighboring wires.^{3,18} Notably, both Au-Si(553) and Au-Si(557) exhibit a complex multiband situation, and all these stepped systems exhibit complex lattice instabilities upon cooling. In chains on Si(111), likewise with a phase transition, also show multiple bands at the Fermi surface and a noticeable undulation for the most 1D-like band, attributed to interband interaction.⁸

The shape of the Fermi contour is suggestive of various *nesting conditions* for a CDW, with distortion vectors $q_1 = 0.12 \text{ \AA}^{-1} \sim 0.15 G$, $q_2 = 0.28 \text{ \AA}^{-1} \sim 0.35 G$, and $q_3 = 0.52 \text{ \AA}^{-1} \sim 0.65 G$ (where $G = 0.80 \text{ \AA}^{-1}$ is the reciprocal translation vector in the 1D direction). None of them appears to be commensurate with the lattice.

The occurrence of a CDW superstructure can be probed with temperature-dependent LEED. The pattern in Fig. 4(a) at 300 K reflects the $c(8 \times 2)$ long-range order. However, at much lower temperatures no additional superstructure is observed, as evident from the LEED results at 10 K in Fig. 4(b). Hence

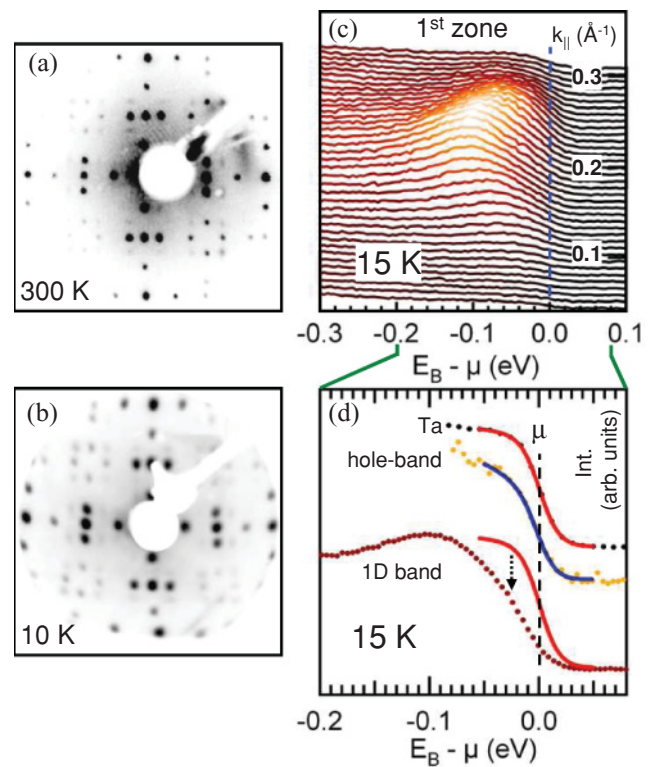


FIG. 4. (Color online) (a) LEED pattern (21 eV) of $c(8 \times 2)$ reconstruction (dual domain) at 300 K. (b) LEED pattern (24 eV) at 10 K. It shows no additional spots so that a CDW is excluded. (c) EDCs of the 1D electron pocket at 15 K (first SBZ). (d) EDCs at 15 K of Ta foil (black dots, aligned with μ) and metallic 2D band [yellow (bright) dots] used for μ determination, fitted with resolution-broadened Fermi function including a linearly sloping density of states [red and blue overlay (solid lines)]. The angle-integrated EDC (0.10–0.30 \AA^{-1}) of the 1D band (lowest dotted line) deviates from the metallic Fermi edges [red (solid) line: Ta Fermi fit overlay], exhibiting suppressed spectral weight within ~ 50 meV below μ .

formation of a CDW that would imply energy gaps can be excluded. This opens the pathway to study the nonperturbed low-energy spectral function of the 1D electron band at low temperature.

In the energy distribution curves (EDCs) of the 1D band at 15 K in Fig. 4(c), no gap opening or band backfolding occurs, although the spectral intensity is rather low near μ . This can be compared to the Fermi edge of the Ta clip in Fig. 4(d). It reflects the experimental resolution (~ 30 meV) and the small thermal broadening ($4kT \sim 5$ meV). The metallic 2D band at \bar{M} (used as an intrinsic reference for μ) closely replicates the Ta Fermi edge, albeit with slightly sloping background. In contrast, the angle-integrated spectrum in Fig. 4(d) covering the whole range of the 1D electron pocket indicates that the spectral weight is unusually suppressed in a range of ~ 50 meV below μ .

Since our investigations exclude a static Peierls distortion, one needs to consider non-Fermi-liquid behavior, where the

spectral weight is predicted to vanish toward μ .⁶ Experimentally this was found, e.g., in lithium purple bronze.²¹ We refrain from further analysis here due to resolution limitations. Hence, it will be insightful to scrutinize the line shape in dedicated high-resolution studies, including the temperature dependence.

In conclusion, the electron system of the Au/Ge(001) chains mapped by ARPES exhibits straight Fermi surface lines, whose 1D character is exceptionally high. At the same time, a CDW can be excluded even at 10 K. The 1D electron topology thus appears to satisfy the requirements for exotic physics. The two electron pockets call for corresponding theoretical modeling and future line shape studies.

The authors are grateful to Y. S. Kim, L. Patthey, and T. Umbach for technical support, and funding by the DFG (Grants No. Scha 1510/3-1 and No. FOR 1162) and DOE (Grant No. DE-AC03-76SF00098).

-
- ¹H. W. Yeom, S. Takeda, E. Rotenberg, I. Matsuda, K. Horikoshi, J. Schaefer, C. M. Lee, S. D. Kevan, T. Ohta, T. Nagao, and S. Hasegawa, *Phys. Rev. Lett.* **82**, 4898 (1999).
- ²P. Segovia, D. Purdie, M. Hengsberger, and Y. Baer, *Nature (London)* **402**, 504 (1999).
- ³J. N. Crain, A. Kirakosian, K. N. Altmann, C. Bromberger, S. C. Erwin, J. L. McChesney, J.-L. Lin, and F. J. Himpsel, *Phys. Rev. Lett.* **90**, 176805 (2003).
- ⁴J. Schäfer, C. Blumenstein, S. Meyer, M. Wisniewski, and R. Claessen, *Phys. Rev. Lett.* **101**, 236802 (2008).
- ⁵G. Grüner, *Density Waves in Solids* (Addison-Wesley, Reading, MA, 1994).
- ⁶J. Voit, *Rep. Prog. Phys.* **58**, 977 (1995).
- ⁷J. R. Ahn, P. G. Kang, K. D. Ryang, and H. W. Yeom, *Phys. Rev. Lett.* **95**, 196402 (2005).
- ⁸J. R. Ahn, J. H. Byun, H. Koh, E. Rotenberg, S. D. Kevan, and H. W. Yeom, *Phys. Rev. Lett.* **93**, 106401 (2004).
- ⁹R. Losio, K. N. Altmann, A. Kirakosian, J.-L. Lin, D. Y. Petrovykh, and F. J. Himpsel, *Phys. Rev. Lett.* **86**, 4632 (2001).
- ¹⁰J. R. Ahn, H. W. Yeom, H. S. Yoon, and I.-W. Lyo, *Phys. Rev. Lett.* **91**, 196403 (2003).
- ¹¹J. Schäfer, D. Schrupp, M. Preisinger, and R. Claessen, *Phys. Rev. B* **74**, 041404(R) (2006).
- ¹²A. A. Stekolnikov, F. Bechstedt, M. Wisniewski, J. Schäfer, and R. Claessen, *Phys. Rev. Lett.* **100**, 196101 (2008).
- ¹³A. Van Houselt *et al.*, *Phys. Rev. Lett.* **103**, 209701 (2009); J. Schäfer *et al.*, *ibid.* **103**, 209702 (2009).
- ¹⁴K. Nakatsuji, R. Niikura, Y. Shibata, M. Yamada, T. Iimori, and F. Komori, *Phys. Rev. B* **80**, 081406(R) (2009).
- ¹⁵J. Schäfer, S. Meyer, C. Blumenstein, K. Roensch, R. Claessen, S. Mietke, M. Klinke, T. Podlich, R. Matzdorf, A. A. Stekolnikov, S. Sauer, and F. Bechstedt, *New J. Phys.* **11**, 125011 (2009).
- ¹⁶S. Hüfner, *Very High-Resolution Photoelectron Spectroscopy* (Springer-Verlag, Berlin, 1998), Chap. 6.
- ¹⁷K. Nakatsuji, Y. Takagi, F. Komori, H. Kusunohara, and A. Ishii, *Phys. Rev. B* **72**, 241308(R) (2005).
- ¹⁸J. N. Crain, J. L. McChesney, F. Zheng, M. C. Gallagher, P. C. Snijders, M. Bissen, C. Gunde lach, S. C. Erwin, and F. J. Himpsel, *Phys. Rev. B* **69**, 125401 (2004).
- ¹⁹S.-J. Tang, T.-R. Chang, C.-C. Huang, C.-Y. Lee, C.-M. Cheng, K.-D. Tsuei, H.-T. Jeng, and C.-Y. Mou, *Phys. Rev. B* **81**, 245406 (2010).
- ²⁰Y. Ohtsubo, S. Hatta, K. Yaji, H. Okuyama, K. Miyamoto, T. Okuda, A. Kimura, H. Namatame, M. Taniguchi, and T. Aruga, *Phys. Rev. B* **82**, 201307 (R) (2010).
- ²¹F. Wang, J. V. Alvarez, S.-K. Mo, J. W. Allen, G.-H. Gweon, J. He, R. Jin, D. Mandrus, and H. Höchst, *Phys. Rev. Lett.* **96**, 196403 (2006).